Conf-930913--48

LA-UR- 94-1087

*Title:*

# A THORIUM/URANIUM FUEL CYCLE FOR AN ADVANCED ACCELERATOR TRANSMUTATION OF NUCLEAR WASTE CONCEPT

*Author(s):*

Michael T. Truebenbach, University of Wisconsin
Douglass L. Henderson, University of Wisconsin
Francesco Venneri, P-17
Edward D. Arthur, ATW, Host Scientist

MASTER

## Los Alamos
NATIONAL LABORATOR

# A THORIUM/URANIUM FUEL CYCLE FOR AN ADVANCED
# ACCELERATOR TRANSMUTATION OF NUCLEAR WASTE CONCEPT

M.T. Truebenbach and D.L. Henderson
University of Wisconsin-Madison
1500 Johnson Drive
Madison, Wisconsin 53706-1687
(608) 263-0808

F. Venneri
Los Alamos National Laboratory
P.O. Box 1663
Los Alamos, NM 87545
(505) 665-5348

## ABSTRACT

Utilizing the high thermal neutron flux of an accelerator driven transmuter to drive a Thorium-Uranium fuel production scheme, it is possible to produce enough energy in the transmuter not only to power the accelerator, but to have enough excess power available for commerical use. A parametric study has been initiated to determine the "optimum" equilibrium operation point in terms of the minimization of the equilibrium actinide inventory and the fuel $\alpha$ for various residence times in the High Flux Region (HFR) and in the Low Flux Region (LFR). For the cases considered, the "optimum" equilibrium operation point was achieved for a HFR residence time of 45 days and a LFR residence time of 60 days. For this case, the total actinide inventory in the system is about 20 tonnes and the fuel $\alpha$ approximately 1.46.

## I. INTRODUCTION

An advanced ATW (Accelerator Transmutation of Nuclear Waste Concept) design, utilizing a Thorium-Uranium fuel cycle, is one of several accelerator driven transmuter concepts under consideration at Los Alamos National Lab rator.[1] The proposed design, as shown in Figure 1, consists of a liquid lead spallation target surrounded by a molten salt, helium cooled, graphite moderated blanket. The goal of this concept is to design a self-contained, self-sufficient transmuter which breeds and burns its own fuel, transmutes its own waste, and produces sufficient energy to power the accelerator and the transmuter's supporting facilities. Excess generating capacity would be placed on the power grid for off site commercial use. The design goal is to have the transmuter/energy producer operate at 3000 $MW_{th}$.

The Thorium/Uranium fuel mixture is slowly circulated through the blanket region in the form of a molten salt solution. The molten salt solution flows through two distinct regions as depicted in Figure 2; the first is a HFR (High Flux Region), a region of intense thermal neutron flux of approximately $2 \times 10^{15}$ neutrons/cm$^2$-s which enhances the production of $^{233}$Pa and the fissioning of $^{233}$U and $^{235}$U. The second region is a LFR (Low Flux Region), a region of low thermal neutron flux which provides a hold-up area for the decay of $^{233}$Pa to $^{233}$U. Part of the molten salt solution is diverted to a separate stream to extract the fission products which have accumulated in the solution. $^{232}$Th is continuously added to the HFR to provide a steady source of fertile fuel.

One of the concerns associated with this advanced concept is the inventory of fissile/fertile material present in the system. Due to safety and nuclear proliferation concerns and to minimize the risk to the environment in case of an accident, it is desired to keep the material inventory at a minimum. However the minimization of the fuel inventory is only one aspect of the design. From a neutron economy and subcritical blanket multiplication factor standpoint, it is desired to minimize parasitic absorption within the molten salt fuel. A measure of the parasitic absorption taking place in the fuel is provided by $\alpha$, the capture-to-fission ratio of the fuel, which affects the subcritical multiplication factor of the transmuter system. A parametric study has been initiated to determine the "optimum" equilibrium operation point in terms of the minimization of the equilibrium actinide inventory and the fuel $\alpha$ for the Thorium/Uranium fuel cycle of the advanced ATW concept for various residence times through the HFR and LFR regions.

## II. METHOD OF SOLUTION

### A. Rate Equations

The actinides comprising the Thorium/Uranium fuel cycle and their interdependency are depicted in Figure 3. The rate equations for the nuclides involved in the fuel cycle form a system of coupled first order linear differential equations which govern the time rate of change of the nuclide densities resulting from radioactive decay and transmutation by neutron absorption. The equations are of the form

$$
\frac{dN_i(\vec{r}, t)}{dt} = \Phi(\vec{r}, t) \times \sum_j N_j(\vec{r}, t) \sigma_{j \to i}(\vec{r})
$$
$$
+ \sum_k N_k(\vec{r}, t) \lambda_{k \to i}
$$
$$
- \Phi(\vec{r}, t) N_i(\vec{r}, t) \times \sum_\ell \sigma_{i \to \ell}(\vec{r})
$$
$$
- N_i(\vec{r}, t) \sum_m \lambda_{i \to m} + S_i(\vec{r}, t) \qquad (1)
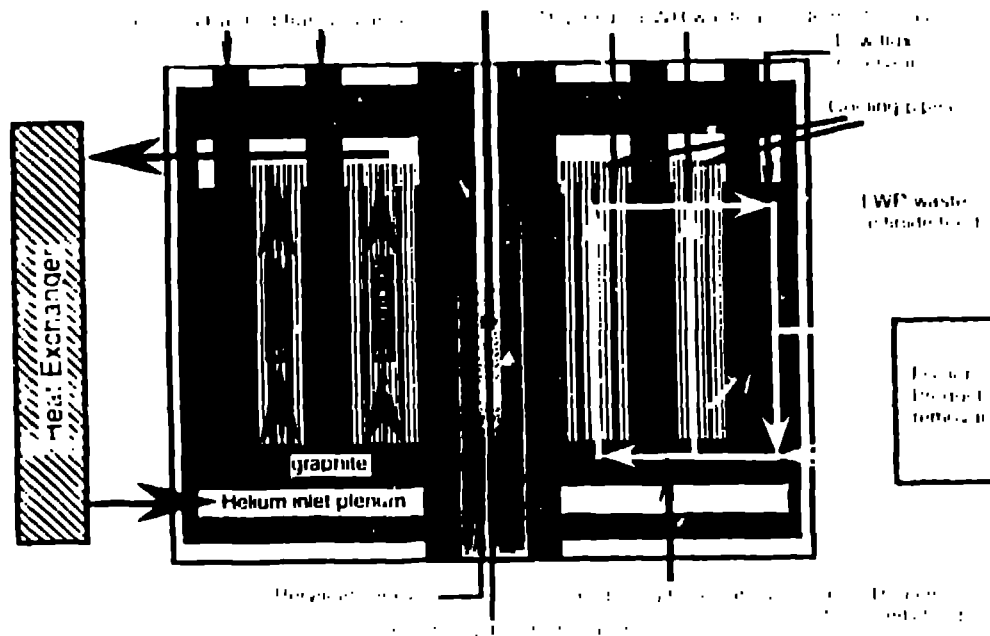$$

1

Figure 1 Schematic of the advanced ATW non-aqueous system blanket region

where:

$N_i(\vec{r},t)$ — number density of nuclide $i$ at time $t$, at position $\vec{r}$;

$\Phi(\vec{r},t)$ = total flux at time $t$, at position $\vec{r}$;

$\sigma_{n \to p}(\vec{r})$ = microscopic cross section for changing nuclide $n$ into nuclide $p$ at position $\vec{r}$;

$\lambda_{q \to s}$ — decay constant for nuclide $q$ changing into nuclide $s$;

$S_i(\vec{r},t)$ = external source of nuclide $i$ at time $t$, at position $\vec{r}$;

and where all references to multigroup fluxes and spectra averaged cross sections have been suppressed. The initial conditions are that $N_i(\vec{r},0) = N_{i,0}(\vec{r})$.

Equation 1 can be cast into a general matrix equation (where the spatial variable has been suppressed).

$$\frac{d\vec{N}}{dt} = A \times \vec{N}(t) + \vec{S}(t) \qquad (2)$$

where

$\vec{N}(t)$ = nuclide density vector
$\quad = [N_1(t), N_2(t), \ldots, N_N(t)]^T$;

$\vec{S}(t)$ = external source vector
$\quad = [S_1(t), S_2(t), \ldots, S_N(t)]^T$.

$A$ · matrix $\{a_{ij}\}$,

$a_{ij}$ $\quad \left(\sigma_i^D \Phi + \lambda_i\right)\delta_{ij} + \left(\sigma_{j \to i}^P \Phi + \lambda_j b_{j \to i}\right)$,

$\sigma_i^D$ · microscopic destruction cross section of nuclide $i$;

$\sigma_{j \to i}^P$ · microscopic production cross section of nuclide $j$ forming nuclide $i$,

$\lambda_i$ decay constant of nuclide $i$,

$b_{j \to i}$ · branching ratio of a decay from nuclide $j$ to nuclide $i$.

$\delta_{ij}$ = the Kronecker delta

Several numerical algorithms have been developed for the solution of large matrix systems as obtained in the above general matrix form. The method employed in this paper to determine the equilibrium actinide concentrations ($^{212}$Th to $^{241}$Am) is a variant of the MEM method (Matrix Exponential Method)[2,3] which we have termed the EMEM method (Eigen value Matrix Exponential Method.[4] As with the standard MEM method, EMEM operates on the general solution of matrix Equation 2. For a time independent external source ($\vec{S}(t) = \vec{S}$) Equation 2 has the solution,

$$\vec{N}(t) = e^{At} \times \vec{N}(0) + \left(I - e^{At}\right) \times A^{-1} \times \vec{S} \qquad (3)$$

where $I$ is the identity matrix, $e^{At}$ is the matrix exponential function and $\vec{N}(0)$ is the initial concentration vector

In the MEM method the matrix exponential function is represented by its series expansion:

$$e^{At} \quad I + \frac{A}{1!}t + \frac{A^2}{2!}t^2 + \frac{A^3}{3!}t^3 + \ldots + \frac{A^n}{n!}t^n + \ldots \qquad (4)$$

To evaluate the exponential function at a specific time $t$, the time period (interval) $t$ is subdivided into time steps of width $\Delta t$. The series in Equation 4 is truncated incorporating sufficient terms so that the answer achieves a specific degree of accuracy at the end of time step $\Delta t$.[1] The computational speed associated with the method is thus dependent on the size of the time step which in turn is dependent on the magnitudes of the destruction rates contained in matrix $A$
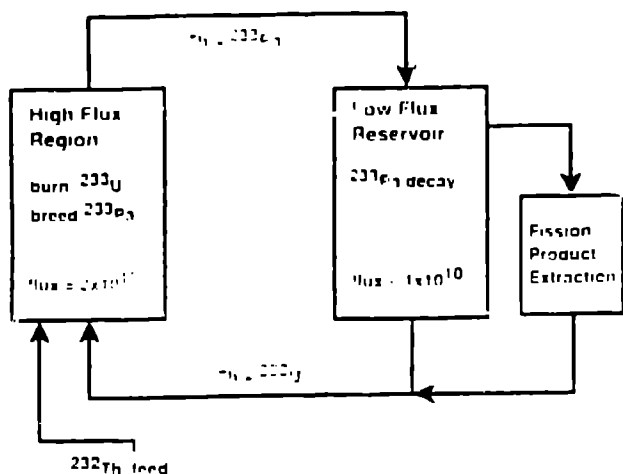
2

Figure 2. Schematic of the material flow through the HFR and LFR regions.



Figure 3. Actinides considered in the Thorium/Uranium fuel cycle and their interdependency.

In the EMEM method the matrix exponential function is decomposed as follows:

$$e^{At} = P \times e^{\Lambda t} \times P^{-1} \qquad (5)$$

where

$$
\begin{aligned}
\Lambda &= \text{diagonal eigenvalue matrix of } A; \\
P &= \text{eigenvector matrix of } A; \\
P^{-1} &= \text{inverse of } P;
\end{aligned}
$$

This decomposition is only valid if matrix A has a complete set of eigenvectors. The exponential matrix function is evaluated explicitly at a specific time $t_e$; no series expansion is necessary or time step control which as noted above increases the computational time. The evaluation of the eigenvalues and eigenvectors of matrix A is greatly simplified if matrix A is written in lower triangular matrix form as is the case for the Thorium/Uranium fuel cycle depicted in Figure 3. For this case the exponential function raised to the diagonal eigenvalue matrix of A has the following form:

$$
e^{\Lambda t} = \begin{bmatrix}
e^{a_{11}t} & 0.0 & 0.0 & \cdots \\
0.0 & e^{a_{22}t} & 0.0 & \cdots \\
0.0 & 0.0 & e^{a_{33}t} & 0.0 \\
\vdots & \vdots & 0.0 & \ddots
\end{bmatrix}
$$

where

$$a_{ii} = -\left(\sigma_i^D \Phi + \lambda_i\right).$$

## B. Equilibrium Concentrations

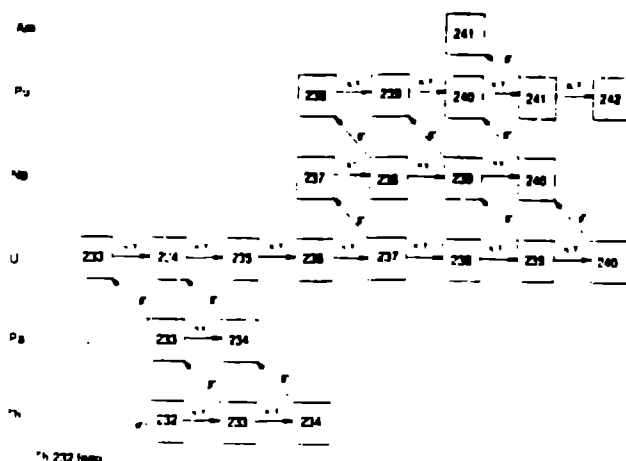Figure 2 depicts a schematic of the molten salt fuel flow through the HFR and LFR regions of the advanced ATW

graphite blanket. The fuel residence time in the HFR region is denoted as $\Delta t_1$ and the time spent in the low flux region is denoted as $\Delta t_2$. The actinide equilibrium concentrations are computed at two locations in the system; the first is at the entrance to the LFR and the second is at the entrance to the HFR. The calculation of the equilibrium concentrations at these two locations is required for the determination of the equilibrium actinide inventory.

It can be shown that after $n$ cycles through the HFR region and $n - 1$ cycles through the LFR region, the actinide concentrations at the entrance to the LFR are given by the expression:

$$
\begin{aligned}
\bar{N}&(n\Delta t_1 + (n-1)\Delta t_2) \\
&= D^{n-1} \times e^{A\Delta t_1} \times \bar{N}(0) \\
&\quad - \left(D^{n-1} + D^{n-2} + \cdots + D + I\right) \\
&\quad \times \left(I - e^{A\Delta t_1}\right) \times A^{-1} \times \bar{S} \qquad (6)
\end{aligned}
$$

where

$$
\begin{aligned}
D &= e^{A\Delta t_1} \times e^{B\Delta t_2}; \\
A &= \text{the radioactive decay/transmutation} \\
&\quad \text{matrix for the HFR}; \\
B &= \text{the radioactive decay/transmutation} \\
&\quad \text{matrix for the LFR}.
\end{aligned}
$$

The equilibrium concentrations of the actinides comprising the radioactive decay/transmutation scheme of Figure 3 which enter the LFR region are obtained as the number of cycles $n$ becomes infinite (i.e. $n \to \infty$). Utilizing the following relationship obtained from the matrix exponential function eigenvalue-eigenvector decomposition of matrix A

$$
\left(I - e^{A\Delta t_1}\right) \times A^{-1} \times \bar{S} =
$$

$$
P \times \left(I - e^{A\Delta t_1}\right) \times \Lambda^{-1} \times P^{-1} \times \bar{S}
$$

and the following limiting values as $n \to \infty$:

$$\lim_{n \to \infty} \left( D^{n-1} \quad D^{n-2} + \cdots + D + I \right) = (I - D)^{-1}$$

and

$$\lim_{n \to \infty} \quad D^{n-1} = 0 .$$

Equation 6 becomes:

$$\overline{N}_{Eq}^{LFR} = -(I - D)^{-1} \times P \times \left( I - e^{I \cdot \Delta t_1} \right)$$
$$\times \quad \Lambda^{-1} \times P^{-1} \times \overline{S}. \quad (7)$$

The expression derived above is for the actinide equilibrium concentrations of the molten salt fuel at the entrance to the LFR region. The actinide equilibrium concentrations at the entrance to the HFR region are computed from the expression:

$$\overline{N}_{Eq}^{HFR} = e^{B \Delta t_2} \times \overline{N}_{Eq}^{LFR}. \quad (8)$$

## C. Equilibrium Inventory Calculation

Now that the equilibrium concentrations have been obtained for a given feedrate, Equations 7 and 8 can be integrated over the time interval that a unit volume of molten salt fuel spends in the HFR and LFR regions. The total inventory of actinide material contained within the HFR is obtained from the integration:

$$\overline{N}_{Inv}^{HFR} = \int_0^{\Delta t_1} [\text{Eq. 3}] dt' = \int_0^{\Delta t_1}$$
$$\left[ e^{A t'} \times \overline{N}(0) - \left( I - e^{A t'} \right) \times A^{-1} \times \overline{S} \right] dt' \quad (9)$$

where $\overline{N}(0)$ holds the equilibrium concentrations entering the HFR region (i.e. $\overline{N}(0) \equiv \overline{N}_{Eq}^{HFR}$). Utilizing the eigenvalue-eigenvector decomposition of matrix A and performing the indicated integration, Equation 9 has the solution:

$$\overline{N}_{Inv}^{HFR} = \quad - \quad P \times \left( I - e^{\Lambda \Delta t_1} \right) \times \Lambda^{-1} \times P^{-1} \times \overline{N}_{Eq}^{HFR}$$
$$- \quad P \times \left[ \Delta t_1 I + \left( I - e^{\Lambda \Delta t_1} \right) \times \Lambda^{-1} \right]$$
$$\times \quad \Lambda^{-1} \times P^{-1} \times \overline{S}. \quad (10)$$

The inventory of actinide material contained in the LFR region is:

$$\overline{N}_{Inv}^{LFR} = -Q \times \left( I - e^{\Gamma \Delta t_2} \right) \times \Gamma^{-1} \times Q^{-1} \times \overline{N}_{Eq}^{LFR} \quad (11)$$

where

$$e^{B \Delta t_2} = Q \times e^{\Gamma \Delta t_2} \times Q^{-1},$$

and

$\Gamma$ = diagonal eigenvalue matrix of B;
$Q$ = eigenvector matrix of B;
$Q^{-1}$ = inverse of Q.

Once the total actinide inventory has been established, the thermal power produced in the HFR is computed. Six nuclides are assumed to contribute to the power of the transmuter, they are, $^{233}U$, $^{235}U$, $^{238}Np$, $^{238}Pu$, $^{239}Pu$ and $^{242}Pu$. Each fissile species is assumed to produce 190 MeV/fission. If the computed thermal power does not equal 3000 MW, then the $^{232}Th$ feedrate is adjusted. Two iterations are required to obtain the actinide total inventory.

D. Calculation of Alpha - The Capture-to-Fission Ratio of the Fuel

The molten salt subcritical blanket multiplication factor, $M$, is related to the neutron multiplication factor, $k$, by the following expression

$$M = \frac{1}{1 - k}$$

where

$$k = \frac{\sum_{i=1}^{N} \nu_i \Sigma_f^i}{\sum_{i=1}^{N} \Sigma_a^i + \Sigma_a^{other}} ;$$

$\Sigma_f^i$ = macroscopic fission cross section of the i'th fuel nuclide.
$\Sigma_a^i$ = macroscopic absorption cross section of the i'th fuel nuclide.
$\Sigma_a^{other}$ = macroscopic absorption cross section of non-fuel constituents, and
$\nu_i$ = the average number of neutrons released per fission for the i'th fuel nuclide.

Defining an effective average number of neutrons released per fission for the fuel $\bar{\nu}$, leads to the following expression for $k$:

$$k = \frac{\bar{\nu}}{1 + \alpha + c}$$

where

$$\bar{\nu} = \frac{\sum_{i=1}^{N} \nu_i \Sigma_f^i}{\sum_{i=1}^{N} \Sigma_f^i} , \quad \alpha = \frac{\sum_{i=1}^{N} \Sigma_\gamma^i}{\sum_{i=1}^{N} \Sigma_f^i} , \text{ and } \quad c = \frac{\Sigma_a^{other}}{\sum_{i=1}^{N} \Sigma_f^i} .$$

We note that $\alpha$ is the ratio of the capture to fission cross sections of the fuel and that it plays an important role in determining $k$ and hence the multiplication, $M$, of the subcritical system. A lower value of $\alpha$ (fewer parasitic absorptions in the fuel) implies a larger value of $k$ which in turn implies a larger value of $M$. All nuclides in the $^{232}Th$ transmutation and decay scheme (see Figure 3) are considered fuel constituents and are included in the calculation of $\alpha$.

E. Data

A brief comment on the data used for the calculations. The molten salt fuel within the advanced ATW system is assumed to
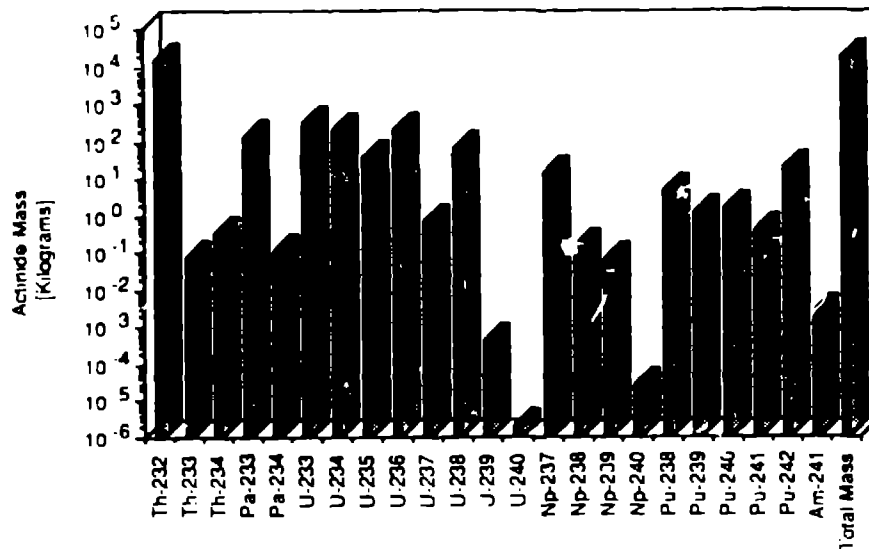
Figure 4  Equilibrium Composition for the 45 day HFR - 90 day LFR residence time case.

Table 1. Actinide Mass Within the ATW System

| Nuclide | 45 HFR/ 90 LFR | 45 HFR/ 150LFR | 30 HFR/ 75 LFR |
|---|---|---|---|
| | Mass [kg] | Mass [kg] | Mass [kg] |
| $^{232}$Th | 1.465e+4* | 2.116e+4 | 1.709e+4 |
| $^{233}$Th | 7.334e-2 | 7.334e-2 | 7.332e-2 |
| $^{234}$Th | 2.952e-1 | 2.953e-1 | 2.954e-1 |
| $^{233}$Pa | 1.191e+2 | 1.200e+2 | 1.208e+2 |
| $^{234}$Pa | 1.0004e-1 | 9.395e-2 | 8.237e-2 |
| $^{233}$U | 2.752e+2 | 4.423e+2 | 2.989e+2 |
| $^{234}$U | 1.946e+2 | 2.737e+2 | 2.094e+2 |
| $^{235}$U | 3.554e+1 | 4.992e+1 | 3.831e+1 |
| $^{236}$U | 1.935e+2 | 2.718e+2 | 2.085e+2 |
| $^{237}$U | 6.564e-1 | 6.385e-1 | 6.204e-1 |
| $^{238}$U | 6.617e+1 | 9.300e+1 | 6.461e+1 |
| $^{239}$U | 3.880e-4 | 3.774e-4 | 3.247e-4 |
| $^{240}$U | 2.053e-6 | 1.937e-6 | 1.718e-6 |
| $^{237}$Np | 1.292e+1 | 1.843e+1 | 1.416e+1 |
| $^{238}$Np | 1.392e-1 | 1.354e-1 | 1.330e-1 |
| $^{239}$Np | 5.704e-2 | 5.549e-2 | 4.807e-2 |
| $^{240}$Np | 2.398e-5 | 2.333e-5 | 1.939e-5 |
| $^{238}$Pu | 4.569e+0 | 6.459e+0 | 5.102e+0 |
| $^{239}$Pu | 1.153e+0 | 1.645e+0 | 1.243e+0 |
| $^{240}$Pu | 1.531e+0 | 2.149e+0 | 1.647e+0 |
| $^{241}$Pu | 3.470e-1 | 4.853e-1 | 3.734e-1 |
| $^{242}$Pu | 1.792e+1 | 2.514e+1 | 1.927e+1 |
| $^{241}$Am | 2.370e-3 | 5.270e-3 | 2.586e-3 |
| Total Mass | 1.558e+4 | 2.247e+4 | 1.808e+4 |
| Fissile Mass | 3.170e+2 | 5.009e+2 | 3.441e+2 |
| $^{232}$Th Feedrate [atoms/s] | 2.54e+13 | 2.54e+13 | 3.81e+13 |

*read as 1.465 × 10^4

be at a temperature of 1500°C. The cross section data utilized for the calculations was taken from MCNP[5] cross section data files at the operating temperature.

## III.  RESULTS

The equilibrium actinide inventories for the advanced ATW concept for a 45 day residence time in the HFR and a 90 day residence time in the LFR (45 HFR/90 LFR) are depicted in Figure 4.  $^{232}$Th dominates the inventory of the system contributing to over 94% of the mass in the system. The large inventory of $^{232}$Th is required for the production of $^{233}$U and to a lesser degree $^{235}$U as they dominate the energy production in the system. A comparison of the actinide inventories for the 45 HFR/90 LFR, 45 HFR/150 LFR and the 30 HFR/75 LFR cases is presented in Table 1. Of the 3 cases presented, the 45 HFR/90 LFR case has the lowest total actinide and fissile inventories.

The percentage of power produced by each fissile isotope considered is presented in Table 2. For all cases presented $^{233}$U produces over 84% of the power followed by $^{235}$U with approximately 13%. Of the other fissile isotopes only $^{239}$Pu contributes more than 1% of the power.

Figure 5 summarizes the 45 day HFR residence time total actinide inventory and fuel α results for varying LFR residence times. As the residence time in the LFR increases the total actinide mass in the system increases (i.e., the inventory of material residing in the LFR increases as the holdup time is increased). We note that α decreases to an asymptotic value as the LFR residence time increases. This reflects the production of $^{233}$U from the decay of $^{233}$Pa in the LFR. Over 98% of the $^{233}$Pa will have decayed to $^{233}$U for a residence time corresponding to six $^{233}$Pa half-lives, hence there is little incentive to increase the holdup time beyond this duration. α decreases because of an increase in $^{233}$U. We note that the minimization of the fuel α and the total actinide mass in the system are in opposing directions. The curves intersect at approximately 60

Table 2. Power Production from Fissile Isotopes

| Nuclide | 45 HFR/90 LFR Power [MW] | 45 HFR/90 LFR Percent of Total [%] | 45 HFR/150 LFR Power [MW] | 45 HFR/150 LFR Percent of Total [%] | 30 HFR/75 LFR Power [MW] | 30 HFR/75 LFR Percent of Total [%] |
|---|---|---|---|---|---|---|
| $^{233}$U | 2525.07 | 84.17 | 2525.07 | 84.17 | 2561.27 | 85 38 |
| $^{235}$U | 408.70 | 13.62 | 408.70 | 13.62 | 377.50 | 12.58 |
| $^{238}$Np | 18.86 | 0 63 | 18.86 | 0.63 | 17.43 | 0.58 |
| $^{238}$Pu | 1.26 | 0.04 | 1.26 | 0.04 | 1.21 | 0.04 |
| $^{239}$Pu | 34.46 | 1.15 | 34.46 | 1.15 | 31.85 | 1.06 |
| $^{241}$Pu | 11.65 | 0.39 | 11.65 | 0.39 | 10.74 | 0.36 |
| Total | 3000.00 | 100.00 | 3000.00 | 100.00 | 3000.00 | 100.00 |



Figure 5. Total actinide mass and fuel $\alpha$ for a 45 day residence time in the HFR and varying residence times in the LFR.
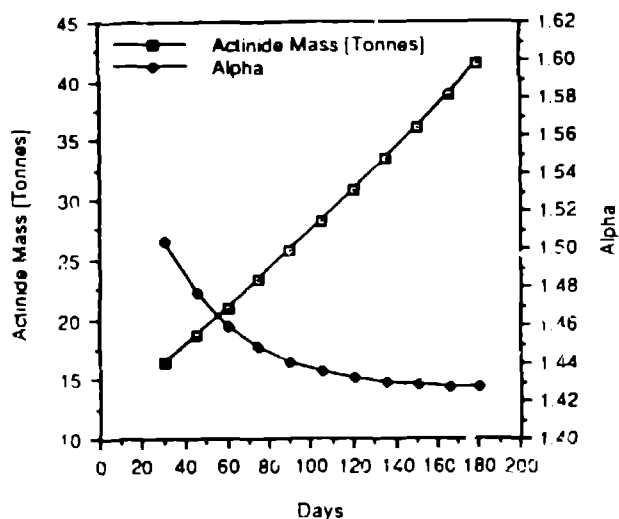


Figure 6. Total actinide mass and fuel $\alpha$ for a 90 day residence time in the LFR and varying residence times in the HFR.

days in the LFR. At this LFR residence time the total actinide inventory in the system is approximately 20 tonnes and the fuel $\alpha$ is about 1.46.

Figure 6 summarizes the 90 day LFR residence time total actinide inventory and fuel $\alpha$ results for varying HFR residence times. We note that the total actinide mass in the system decreases as the residence time in the HFR increases. The reason for this is that $\alpha$ the residence time in the HFR increases more of the $^{233}$Pa decays to $^{233}$U while still residing in the HFR. However $\alpha$ increases as the residence time in the HFR increases due to parasitic absorption in Pa and higher mass U isotopes in the fuel. For the specific case of 90 days in the LFR, the total actinide mass and $\alpha$ curves intersect at approximately 60 days in the HFR. The total actinide inventory and $\alpha$ values are approximately 22.5 tonnes and 1.47, respectively.

## IV. SUMMARY

A parametric study has been initiated to determine the "optimum" equilibrium operation point in terms of the minimization of the minimum equilibrium actinide inventory and
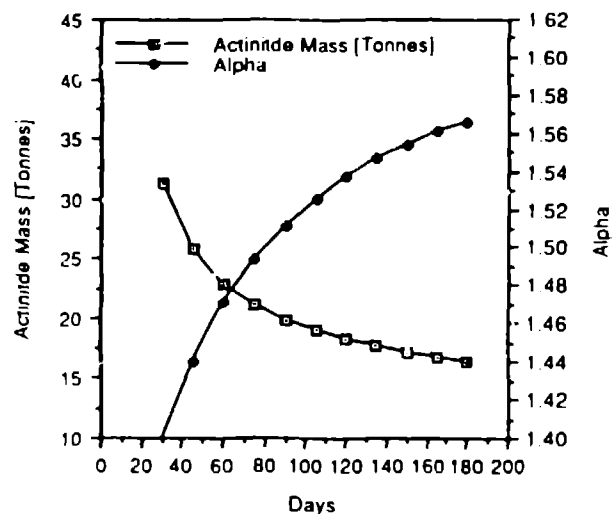
the fuel $\alpha$ for various residence time through the HFR and LFR regions of the advanced ATW concept. From the results of this study, the minimization of $\alpha$ and the total actinide inventory in the system are in opposing directions. For the cases considered, the "optimum" equilibrium operation point was achieved for a HFR residence time of 45 days and a LFR residence time of 60 days. At this operation point, the total actinide inventory in the system is about 20 tonnes and the fuel $\alpha$ approximately 1.46. The next step in the analysis of the advanced ATW concept is to include additional Americium and Curium isotopes and to investigate the actinide inventories and fuel $\alpha$ during the equilibration phase of the transmuter.

A brief note about the computer program. The computer code developed for this parametric study utilizes the Eigenvalue Matrix Exponential Method for the solution of the system of first order differential equation which govern the actinide concentrations in the system. The method has proven itself to be computational efficient; no time step control or series expansion is necessary. Radioactive decay loops were not considered in the fuel cycle analysis, they can be easily incorporated along the lines of the Avalanche method.[6]

## REFERENCES

1. F. VENNERI, "ATW Non-Aqueous System Neutronics Design," LA-UR-92-2020, Los Alamos National Laboratory (April 1992).

2. S.J. BELL and R.K. ADAMS, "MATEXP: A General Purpose Digital Computer Program for Solving Ordinary Differential Equations by the Matrix Exponential Method," ORNL-TM-1933, Oak Ridge National Laboratory (1967).

3. A.G. CROFF, "ORIGEN2 – A Revised and Updated Version of the Oak Ridge Isotope Generation and Depletion Code," ORNL-5621, Oak Ridge National Laboratory (July 1980).

4. H. FUKUMOTO, "New Approach to Neutron-Induced Transmutation, Radioactivity and Afterheat Calculations and Its applications to Fusion Reactors," J. Nucl. Sci. and Tech., 23, 97 (1986).

5. J.F. BREISMEISTER, Editor, "MCNP - A General Monte Carlo Code for Neutron and Photon Transport, Version 4," LA-7396-M, Los Alamos National Laboratory (Revised April 1991).

6. D.R. HARRIS, P.T. STANLEY and E. PILAT, "The Avalanche Method and Nd-Pm-Sm Chain Representations," Topical Meeting on Reactor Physics and Shielding, September 17-19, 1984, Chicago, IL (1984).